Electronic Supplementary Material (ESI) for Dalton Transactions.

[Supporting Information]

An unprecedented $[\{Fe_5O_5(OH)_2(OAc)_2\}_2\{W_2O_2(OH)\}]$ cluster sandwiched in the tetravacant tungstophosphate

Zongfei Yang, Yaping Wang, Zhijie Liang, Jingkun Lu, Pengtao Ma, Jingyang Niu,* and Jingping Wang*

Henan Key Laboratory of Polyoxometalate Chemistry, Institute of Molecular and Crystal Engineering, College of Chemistry and Chemical Engineering, Henan University, Kaifeng 475004, Henan (P.R. China)
E-mail: jyniu@henu.edu.cn, jpwang@henu.edu.cn, Fax: (+86)371-23886876

CONTENTS

Section 1 Experimental section

1.1 Materials and methods

$K_{12}[H_2P_2W_{12}O_{48}]\cdot 24H_2O$ was synthetized using literature methods and successfully characterized by IR spectrum.[S1] The others were commercially purchased and used without further purification. Infrared (IR) spectra of compound **1** was recorded on a Bruker Vertex 70 IR spectrometer from solid sample palletized with KBr in the range of 4000–450 cm^{-1}. Thermogravimetric analyses (TGA) were conducted using a Mettler–Toledo TGA/SDTA 851^{e} instrument under a flowing N_2 atmosphere with a heating rate of 10 °C min^{-1} from 25 to 600 °C. Powder X-ray diffraction (PXRD) patterns were collected on a Bruker AXS D8 Advance diffractometer instrument with Cu Kα radiation ($\lambda = 1.54056$ Å) at 293 K. ICP analyses were obtained with a PerkinElmer Optima 2000 ICP–OES spectrometer. C, H and N elemental analyses were performed on a Perkin–Elmer 2400–II CHNS/O analyzer. Magnetic properties of compound **1** were conducted on the Quantum Design SQUID magnetometer (MPMS−VSM) in the range of 1.8–300 K. UV spectra were obtained with a U-4100 spectrometer at room temperature. All electrospray-ionization mass spectrometry (ESI-MS) measurements were performed on an AB SCIEX Triple TOF 4600 spectrometer operating in negative ion mode and data was analyzed using the Peakview 2.0 software provided. The sample was prepared as described in the following and injected directly at a flow rate of 5 µL□min^{-1} using a syringe pump.

1.2 Synthetic

$K_{12}[H_2P_2W_{12}O_{48}]\cdot 24H_2O$ (0.82 g,0.21 mmol) was solubilized in a mixture of 4M NaOAc (6 mL) + H_2O (40 mL) with pH=7.79, and the pH value of the solution became 7.43. Then it was heated to 38°C. $FeCl_3\cdot 6H_2O$ (0.11 g, 0.68 mmol) and $PrCl_3\cdot 7H_2O$ (0.15g, 0.62 mmol) was added in turn giving an earthy yellow suspension (pH=5.98). Finally, the resulting mixture was heated to 95°C for 3h. After this period, the mixture was gradually cooled to room temperature, filtered and then was kept in air for slow evaporation at room temperature. The pH value of the filtrate after the reaction is 5.81. After two months, the reddish brown crystals of compound **1** were obtained. Yield: 0.31g (8.25% Based on W). IR (KBr-pellet): 1086, 1069, 1004, 943, 901, 808, 735, 672 cm^{-1}. Elemental analysis (%) calculated (found) for compound **1**: C 1.03 (1.04), H 1.09 (0.93), K 1.26 (1.28), Na 0.98 (1.00), P 1.33 (1.20), W 59.24 (58.56), Fe 5.98 (5.78).

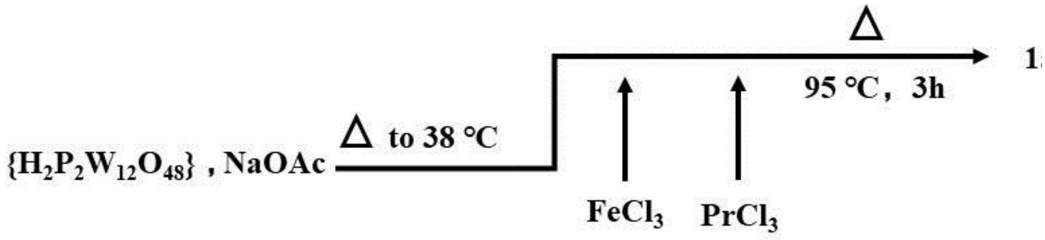

Fig. S1 The experimental process.

1.3 X-ray Crystallography

Table S1. Crystal data and structure refinement for compound **1**

Empirical formula	$C_8H_{101}Fe_{10}K_3Na_4O_{169}P_4W_{30}$
Formula weight	9308.59
Temperature/K	296.15
Crystal system	triclinic
Space group	*P-1*
a/Å	13.4742(6)
b/Å	26.3391(11)
c/Å	31.1489(13)
α/°	114.9234(6)
β/°	95.2570(7)
γ/°	96.9183(7)
Volume/Å^3	9826.9(7)
Z	2
ρ/g·cm^{-3}	3.078
μ/mm^{-1}	18.389
F(000)	7994.0
Crystal size/mm^3	0.33 × 0.16 × 0.14
Radiation	Mo Kα (λ = 0.71073)
range for data collection	3.116 to 50.198
Index ranges	$-15 \leq h \leq 16$, $-25 \leq k \leq 31$, $-37 \leq l \leq 35$
Reflections collected	51307
Independent reflections	34716 [$R_{int} = 0.0443$, $R_{sigma} = 0.0974$]
Data/restraints/parameters	34716/2/1140
Goodness-of-fit on F^2	1.024
Final R indexes [I>=2σ (I)]	$R_1 = 0.0572$, $wR_2 = 0.1449$
Final R indexes [all data]	$R_1 = 0.0992$, $wR_2 = 0.1711$

Section 2 Supplementary tables and structural figures

Table S2 Bond valence sum calculations of all the oxygen atoms of compound **1**.

Atom label	Bond valence Sum	Atom label	Bond valence Sum	Atom label	Bond valence Sum	Atom label	Bond valence Sum
O1	2.031	O36	2.033	O69	1.640	O102	1.834
O2	2.091	O37	1.963	O70	1.966	O103	2.097
O3	1.795	O38	2.093	O71	2.058	O104	1.958
O4	1.837	O39	1.404	O72	2.038	O105#	0.907
O5	1.639	O40	2.084	O73	2.096	O106	1.982
O6	1.877	O41	1.542	O74	1.618	O107	1.923
O7	1.754	O42	2.039	O75	1.957	O108	2.029
O8	2.061	O43	1.845	O76	1.528	O109	1.850
O10	1.699	O44	2.064	O77	1.859	O110	2.042
O11	1.793	O45	1.991	O78	1.891	O111	1.917
O12	1.653	O46	2.058	O79	1.978	O112	1.829
O13	1.887	O47	2.008	O80	1.882	O113	1.864
O14	2.024	O48	1.810	O81	1.971	O114	2.041
O16	1.644	O49	1.861	O82	1.829	O115	1.931
O17	1.867	O50	1.963	O83	2.051	O116	2.048
O18	1.907	O51	2.000	O84#	1.027	O117	1.905
O19	1.592	O52	1.924	O85	1.959	O118	1.979
O20	1.941	O53	1.751	O86	2.106	O119	1.865
O21	1.735	O54	1.914	O87	2.069	O120	1.909
O22	1.520	O55	1.944	O88	1.841	O121	2.095
O23	1.657	O56	2.021	O89	1.911	O122	1.879
O24	2.095	O57	1.833	O90	1.906	O123	1.816
O25	2.039	O58	1.818	O91#	1.063	O124	1.852
O26	1.592	O59	1.570	O92	1.924	O125	2.104
O27	1.986	O60	1.793	O93	1.549	O126	1.779
O28	1.818	O61	1.676	O94	2.036	O127	2.185
O29	1.671	O62	2.104	O95#	1.016	O128	2.034
O30	1.749	O63	1.890	O96	1.869	O129	1.848
O31	2.064	O64	1.994	O97	1.963	O130	1.901
O32	1.764	O65	1.981	O98	1.895	O131#	1.130
O33	1.985	O66	1.717	O99	1.880	O132	1.840
O34	1.923	O67	1.821	O100	1.826	O133	1.884
O35	1.635	O68	2.017	O101	1.834	O134	1.902

#represents mono-pronated groups.

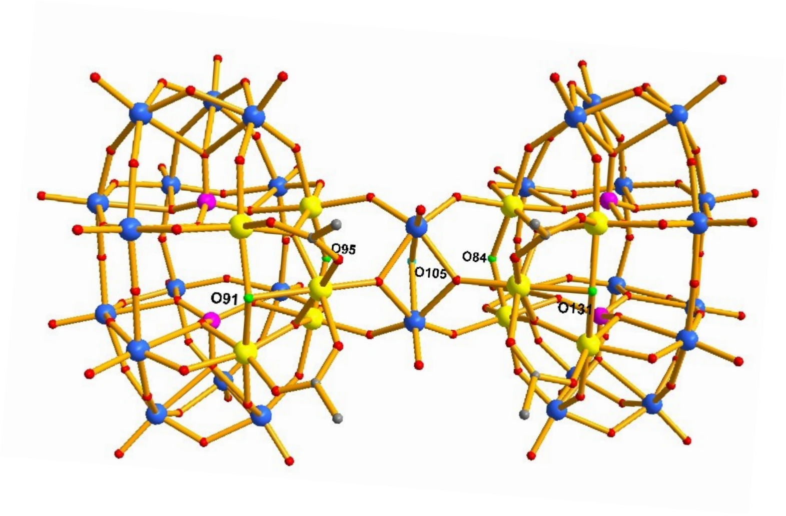

Fig. S2 Ball-and-stick representation of **1a** highlighting the pronated oxygen atoms. Color code: W, light blue balls; P, pink balls; Fe, yellow balls; C, gray-40%; O, red balls; OH, light green balls.

In order to determine the possible positions of the protons, bond valence sum (BVS) calculations are carried out on the all oxygen atoms in **1**. (Table S2, Fig. S2) The BVS calculations give the values of 1.03, 1.06, 1.02, 0.91, 1.13 for O84, O91, O95, O105, O131, respectively, which are relatively lower than those of other oxygen atoms in **1a** and further indicate they are monoprotonated.

Table S3 Bond valence sum calculations of W, Fe and P atoms of compound **1**.

Atom label	Band valence sum	Atom label	Band valence sum	Atom label	Band valence sum	Atom label	Band valence sum
W1	6.146	W12	6.281	W23	6.029	Fe4	3.041
W2	6.175	W13	6.237	W24	6.391	Fe5	3.124
W3	6.426	W14	6.119	W25	5.876	Fe6	3.169
W4	5.999	W15	6.081	W26	6.334	Fe7	3.074
W5	6.424	W16	6.269	W27	6.330	Fe8	2.961
W6	5.831	W17	6.136	W28	6.261	Fe9	2.959
W7	6.175	W18	6.431	W29	6.057	Fe10	2.955
W8	6.084	W19	6.177	W30	6.357	P1	4.845
W9	6.171	W20	6.107	Fe1	3.089	P2	5.081
W10	6.249	W21	6.353	Fe2	3.002	P3	4.823
W11	6.035	W22	6.324	Fe3	3.041	P4	4.870

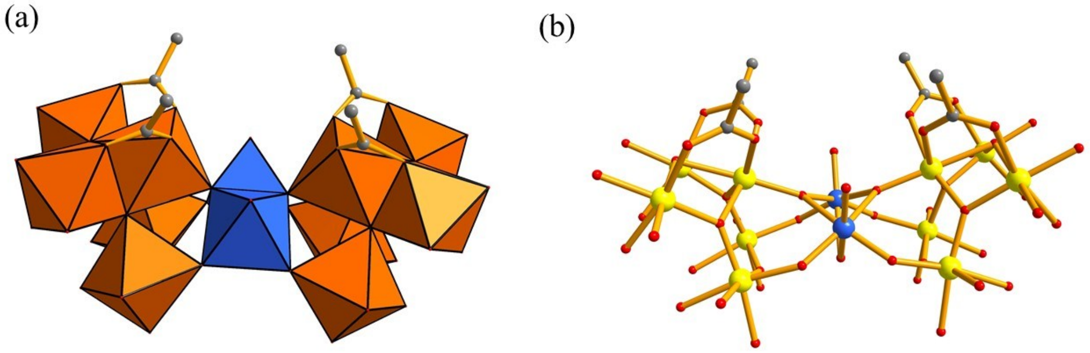

Fig. S3 Polyhedral and ball-and-stick representations of the $[\{Fe_5O_5(OH)_2(OAc)_2\}_2\{W_2O_2(OH)\}]$ cluster. Color code: WO_6 octahedra, light blue; FeO_6 octahedra, orange; W, light blue balls; P, pink balls; Fe, yellow balls; C, gray-40%; O, red balls.

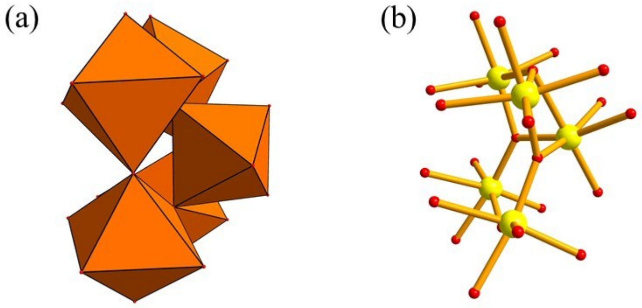

Fig. S4 Polyhedral and ball-and-stick representations of $\{Fe_5\}$.

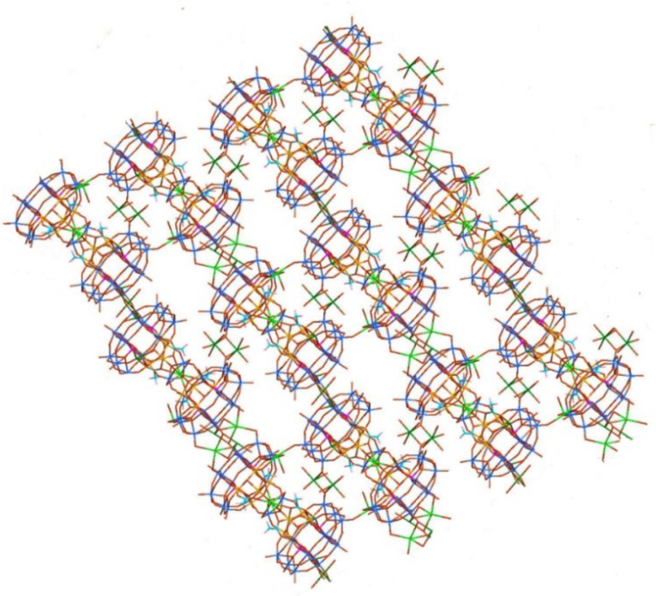

Fig. S5 View of supramolecular three-dimensional structure of **1** with potassium and sodium ions in a axis.

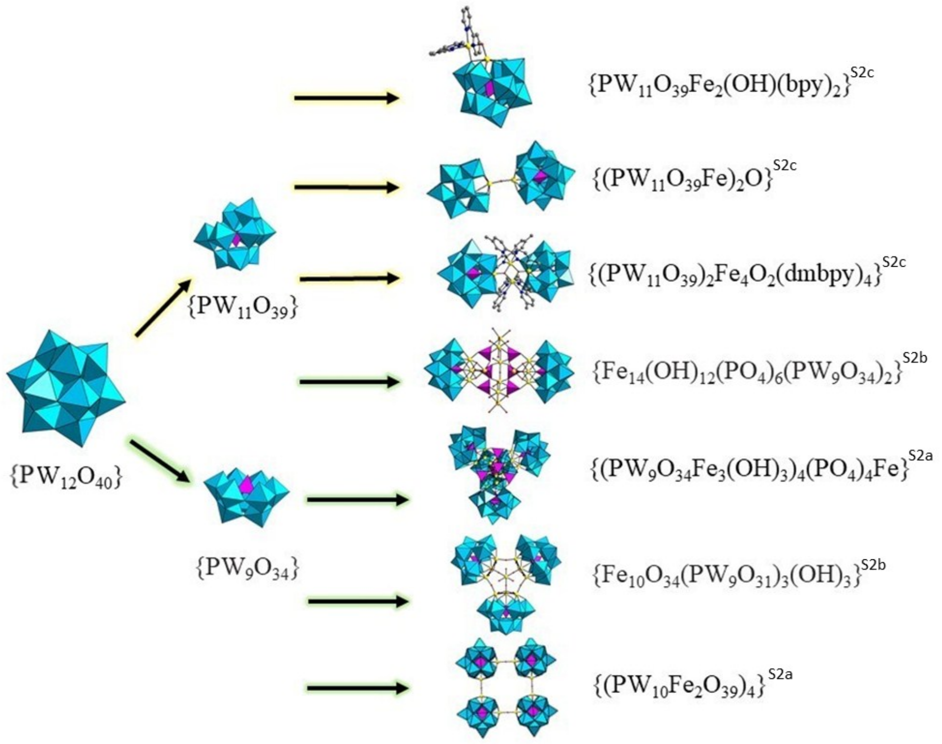

Fig. S6 The summary of the reported lacunary $\{PW_{12}O_{40}\}$ derivatives involving multinuclear ferric ions.[S2]

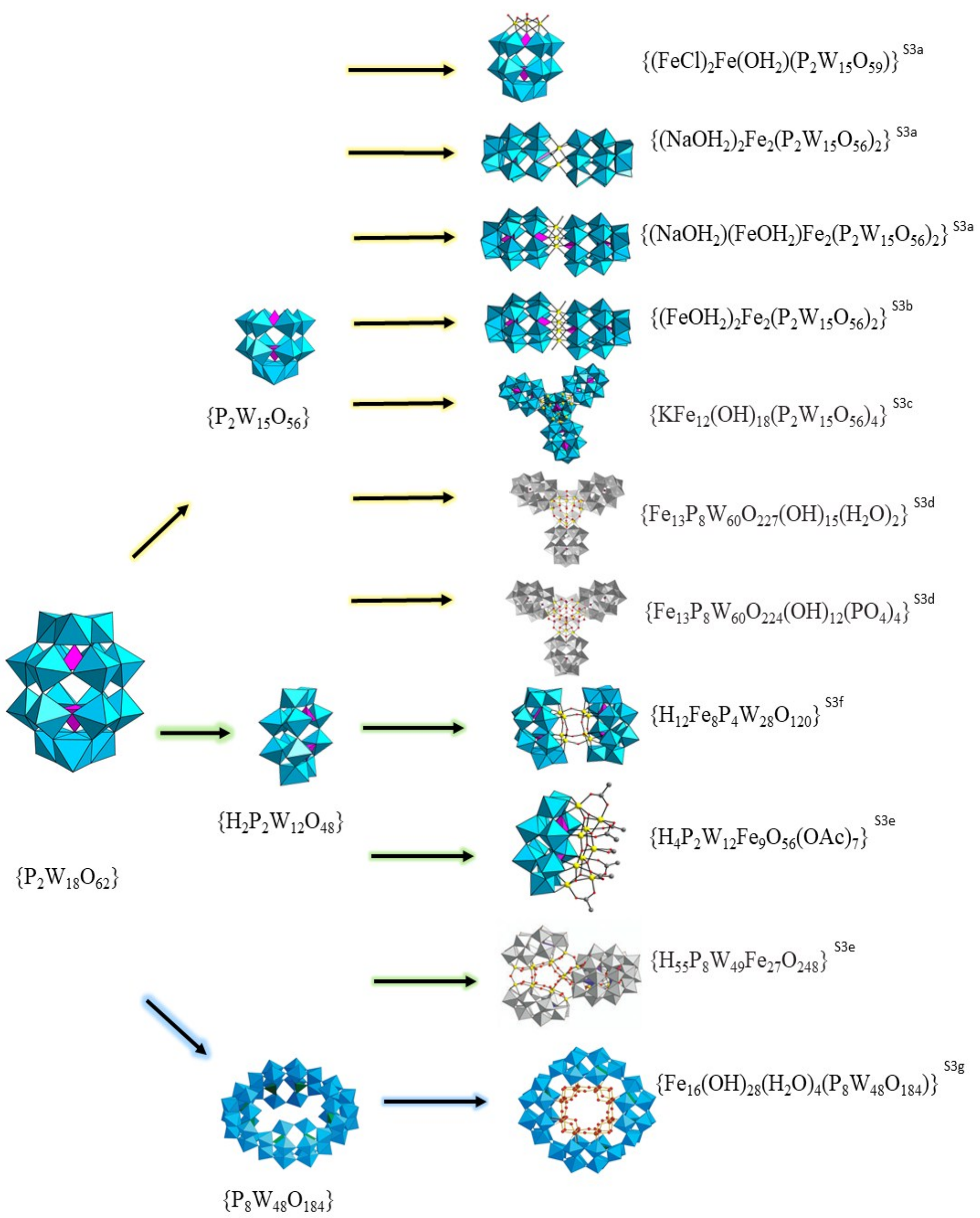

Fig. S7 The summary of the reported lacunary $\{P_2W_{18}O_{62}\}$ derivatives involving multinuclear ferric ions.[S3]

Section 3 Additional measurements

3.1 X-ray powder pattern

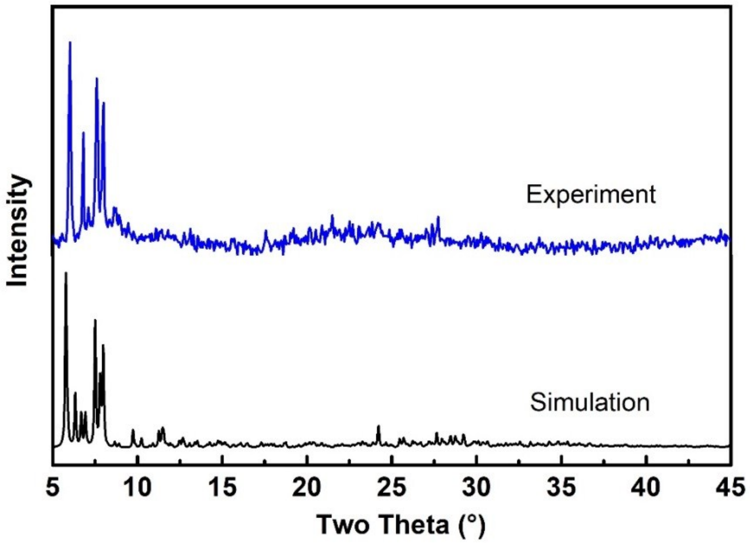

Fig. S8 X-ray powder patterns of compound **1**.

The experimental XRPD patterns agree well with the simulated pattern thus confirms the phase purity in cluster **1**.

3.2 IR spectrum

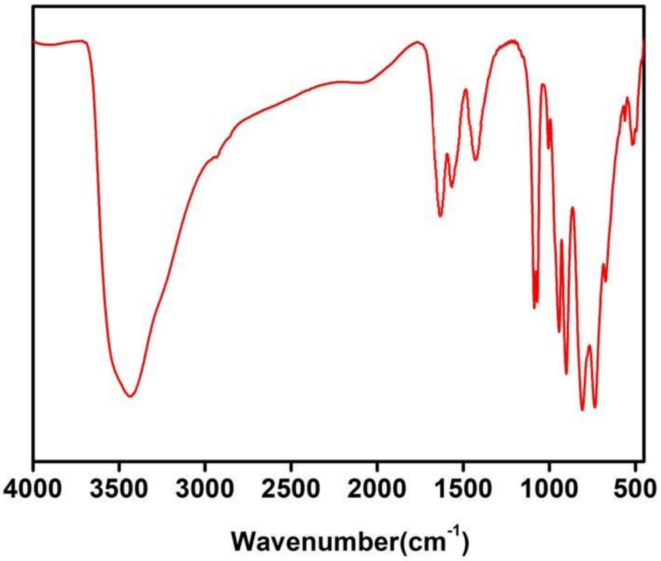

Fig. S9 The IR spectra of **1**.

3.3 TGA analysis

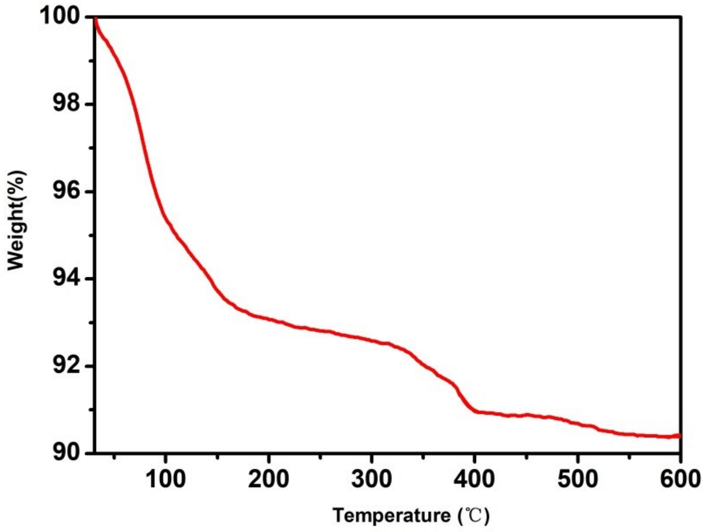

Fig. S10 Thermogravimetric curve of **1**.

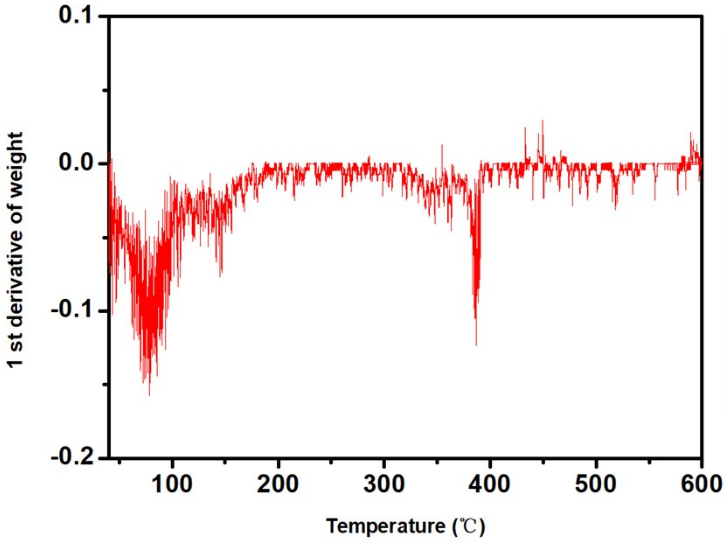

Fig. S11 The first derivative of the weight loss curve vs. T.

The thermal behavior of **1** has been investigated under nitrogen atmospheres between 30 and 600°C by thermogravimetric analysis (TGA). The TGA curve shows two-step weight losses. The first weight loss in the range of 30 - 200 ℃ giving a total loss of 6.90 % (calcd 6.85 %), attributed to the removal of 36 lattice water molecules. The second weight loss of 2.45 % (calcd 2.24 %), which correspond to the oxidation of acetate ligands.[S4]

3.4 Magnetism

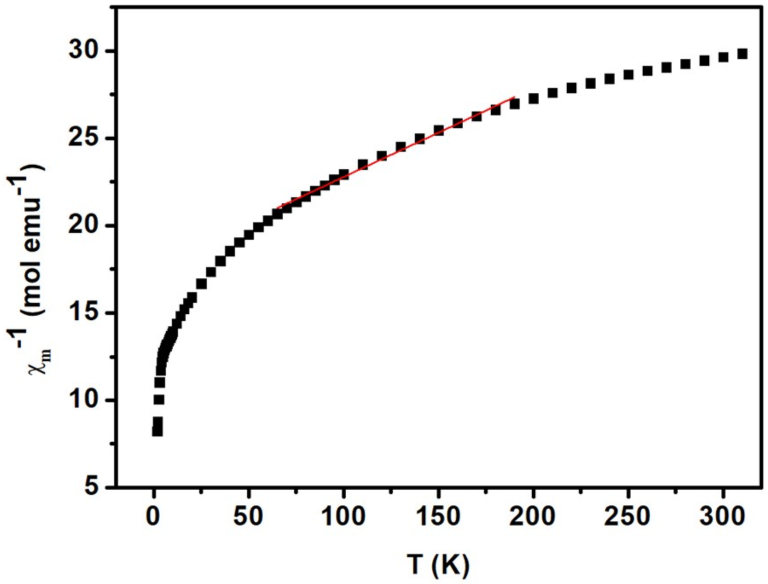

Fig. S12 The temperature dependence of $1/\chi_m$ for **1**, and the red solid for **1** line represent the best-fit by the Curie-Weiss law.

3.5 UV-Vis spectra

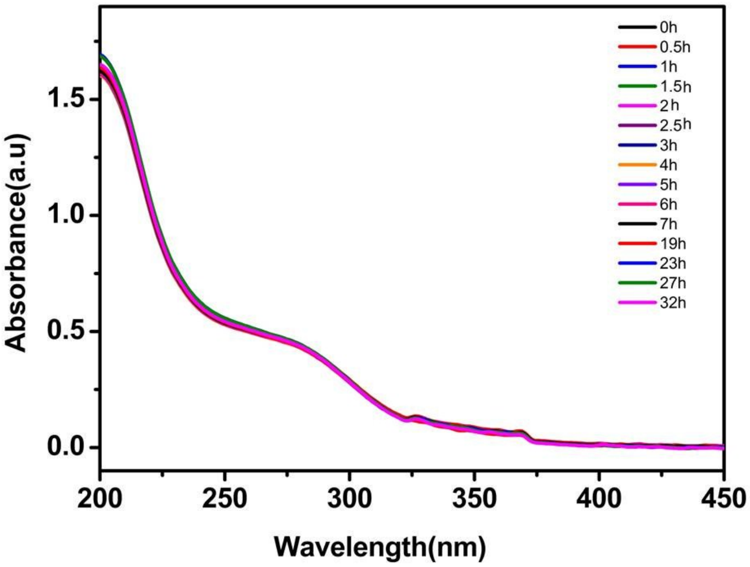

Fig. S13 The time-dependent UV-Vis spectra of compound **1** in the mixed solution of CH_3CN and H_2O ($V(H_2O) : V(CH_3CN) = 1 : 1$).

3.6 ESI-MS

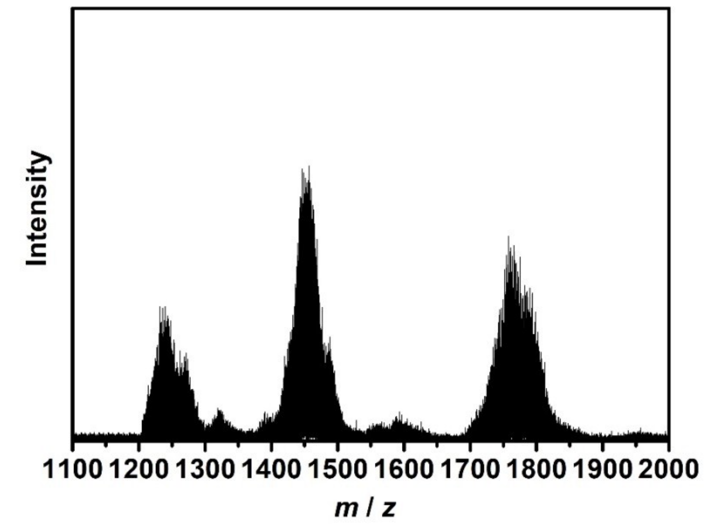

Fig. S14 Negative-mode ESI of compound **1** in a mixed solvent of CH_3CN and H_2O (V (H_2O)/V (CH_3CN) = 1:1).

Table S4 Assignment of mass spectral data for compound **1**.

Charge	Entry	Polyanion	Calculated *m/z*	Observed *m/z*
-5	1	$\{H_{11}Na_2K\mathbf{1a}(H_2O)_3\}^{5-}$	1749.78	1749.50
	2	$\{H_{11}NaK_2\mathbf{1a}(H_2O)_5\}^{5-}$	1760.21	1760.11
	3	$\{H_7Na_4K_3\mathbf{1a}\}^{5-}$	1763.00	1763.25
	4	$\{H_8Na_4K_2\mathbf{1a}(H_2O)_3\}^{5-}$	1766.20	1766.53
-6	1	$\{H_{13}\mathbf{1a}(H_2O)\}^{6-}$	1438.30	1438.32
	2	$\{H_{13}\mathbf{1a}(H_2O)_2\}^{6-}$	1441.30	1441.31
	3	$\{H_{12}K\mathbf{1a}\}^{6-}$	1441.65	1441.64
	4	$\{H_{10}NaK_2\mathbf{1a}\}^{6-}$	1451.66	1451.78
-7	1	$\{H_{12}\mathbf{1a}(H_2O)\}^{7-}$	1232.68	1232.76
	2	$\{H_{11}K\mathbf{1a}(H_2O)_2\}^{7-}$	1240.70	1240.45
	3	$\{H_9Na_2K\mathbf{1a}(H_2O)\}^{7-}$	1244.40	1244.65

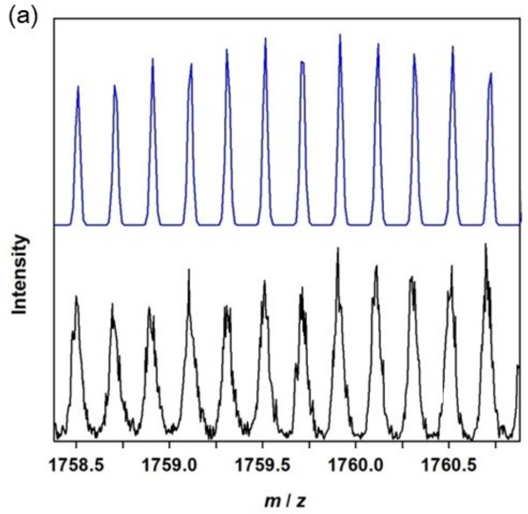

$\{H_{11}NaK_2\mathbf{1a}(H_2O)_5\}^{5-}$

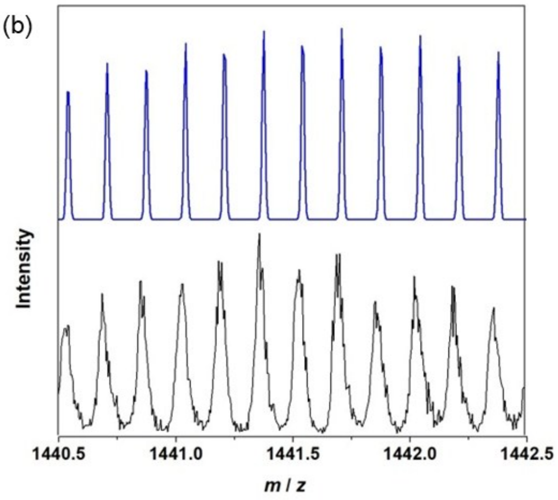

$\{H_{12}K\mathbf{1a}\}^{6-}$

Fig. S15 Selected simulated (blue) and experimental (black) negative-mode mass spectra of the isotopic envelopes for **1**.

Section 4 References

S1 R. Contant, W. G.Klemperer and O. Yaghi O. *Inorg. Synth*. 1990, **27**,104.

S2 (a) C. Pichon, A. Dolbecq, P. Mialane, J. Marrot, E. Rivière and F. Sécheresse, *Dalton Trans.* 2008, 7, 71. (b) V. Singh, Z. Chen, P. Ma, D. Zhang, M. G. B. Drew, J. Niu and J. Wang, *Chem. – Eur. J.* 2016, 22, 10983. (c) C. Pichon, A. Dolbecq, P. Mialane, J. Marrot, E. Rivière, M. Goral, M. Zynek, T. McCormac, S.

A. Borshch and E. Zueva, *Chem. – Eur. J.* 2008, 14, 3189.

S3 (a) B. Keita, I. M. Mbomekalle, L. Nadjo, T. M. Anderson and C. L. Hill, *Inorg. Chem.* 2004, 43, 3257. (b) X. Zhang, T. M. Anderson, Q. Chen and C. L. Hill, *Inorg. Chem.* 2001, 40, 418. (c) C. P. Pradeep, D.-L. Long, P. Kögerler and L. Cronin, *Chem. Commun.* 2007, 41, 4254. (d) P. I. Molina, H. N. Miras, D.-L. Long and L. Cronin, *Dalton Trans.* 2014, 43, 5190. (e) B. Godin, Y.-G. Chen, J. Vaissermann, L. Ruhlmann, M. Verdaguer and P. Gouzerh, *Angew. Chem., Int. Ed.* 2005, 44, 3072. (f) B. Godin, J. Vaissermann, P. Herson, L. Ruhlmann, M. Verdaguer and P. Gouzerh, *Chem. Commun.* 2005, 45, 5624. (g) S. S. Mal, M. H. Dickman, U. Kortz, A. M. Todea, A. Merca, H. Bögge, T. Glaser, A. Müller, S. Nellutla and N. Kaur, *Chem. – Eur. J.* 2008, 14, 1186.

S4 M. Han, Y. Niu, R. Wan, Q. Xu, J. Lu, P. Ma, C. Zhang, J. Niu and J.Wang, *Chem. – Eur. J.* 2018, **24**, 11059.